Cell Reports, Volume *28*

Supplemental Information

Skeletal Stem Cell-Schwann Cell Circuitry in Mandibular Repair

R. Ellen Jones, Ankit Salhotra, Kiana S. Robertson, Ryan C. Ransom, Deshka S. Foster, Harsh N. Shah, Natalina Quarto, Derrick C. Wan, and Michael T. Longaker

Supplemental Figure 1

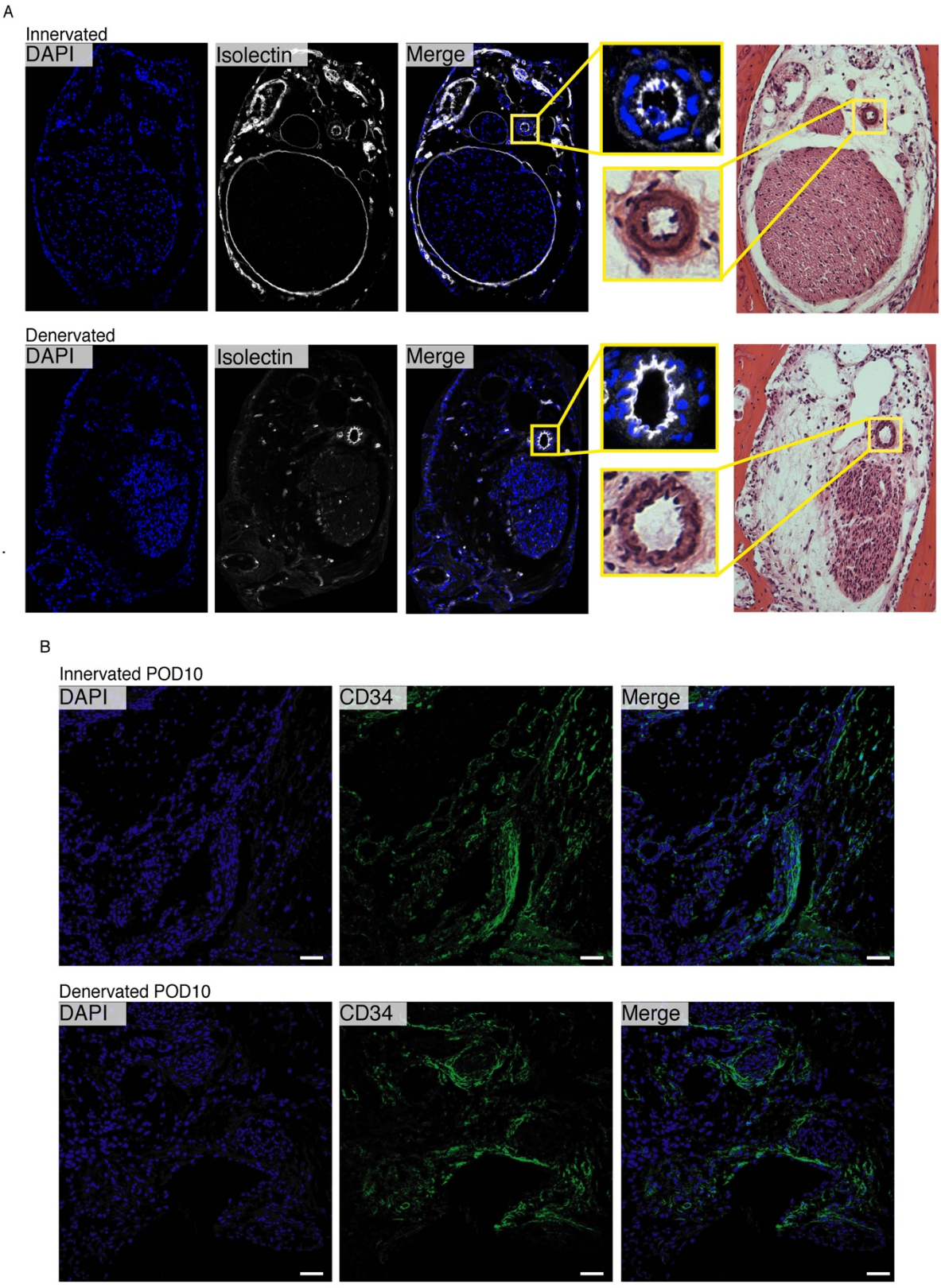

Supplemental Figure 1. Related to Figure 2. Histologic examination of vascular and hematopoietic contribution to nerve dependent mandibular healing.

(A) Tissue sections after *in vivo* administration of isolectin to mark endothelial and epineural cells in the mandibular canal of an uninjured (top panels) and denervated (bottom panels) mandible 2 weeks after surgery. The innervated specimens (top panels) reveal intact nerve and arterial architecture as evidenced by isolectin staining. The artery that travels alongside the IAN inside the mandibular canal is indicated by the yellow box and zoomed to show greater detail. The denervated specimens (bottom panels) reveal degenerated nerves which no longer show isolectin staining. However, the inferior alveolar artery is still intact, as noted in the yellow box, where isolectin staining is observed. Therefore, both conditions show an intact arterial lumen, indicating preserved vascular inflow to the mandible. To the right, hematoxylin and eosin stains of the same representative specimens are shown for reference, with yellow box again indicating the inferior alveolar artery. This experiment was performed with 5 biological replicates per condition. (B) Immunohistochemistry to identify CD34 positive cells (green) in innervated mandible defects (upper panels) and denervated mandible defects (lower panels). DAPI was used as a counterstain (blue). Experiment performed with 5 biological replicates per condition.

Scale bars, 50 μm for IHC staining and 200 μm for HE staining (A), 25 μm for IHC staining and 100 μm for HE staining (A, zoomed inset), 50 μm (B). Harvests performed 2 weeks after denervation (A) and 10 days after mandibular defect creation (B).

Supplemental Figure 2

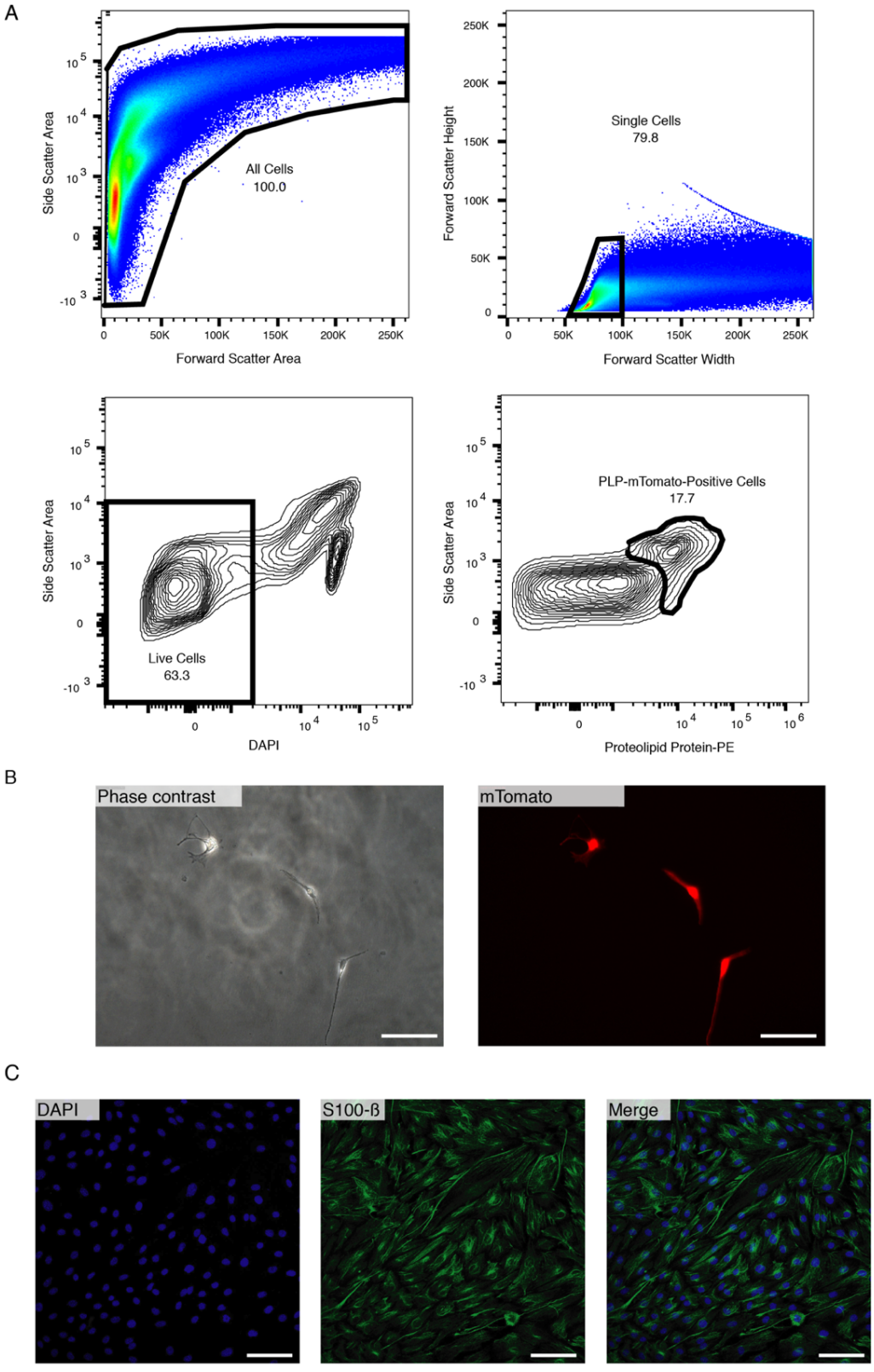

Supplemental Figure 2. Related to Figure 4. Fluorescent activated cell sorting strategy to isolate *PLP*-mTomato-positive Schwann cells and validation.

(A) Gating strategy for FACS isolation of *PLP*-mTomato-positive Schwann cells after digestion of mandibles from PLP Tomato mice. Single cells were determined using forward scatter measurements (top right), and dead cells were excluded with DAPI positivity (bottom left). *PLP*-mTomato positivity was determined by identifying the phycoerythrin (PE)-positive population (bottom right).

(B) Images of *PLP*-mTomato-positive Schwann cells isolated via FACS and grown in culture for 1 week. Typical Schwann cell morphology was noted with phase contrast (left) and *PLP*-mTomato positivity was confirmed with red fluorescence expression (right).

(C) Validation of *PLP*-mTomato-positive Schwann cells was performed with immunocytochemistry. FACS-isolated Schwann cells were stained with S100-ß (green) and counterstained with DAPI (blue).

Scale bars, 100 μm (B, C).

Supplemental Figure 3

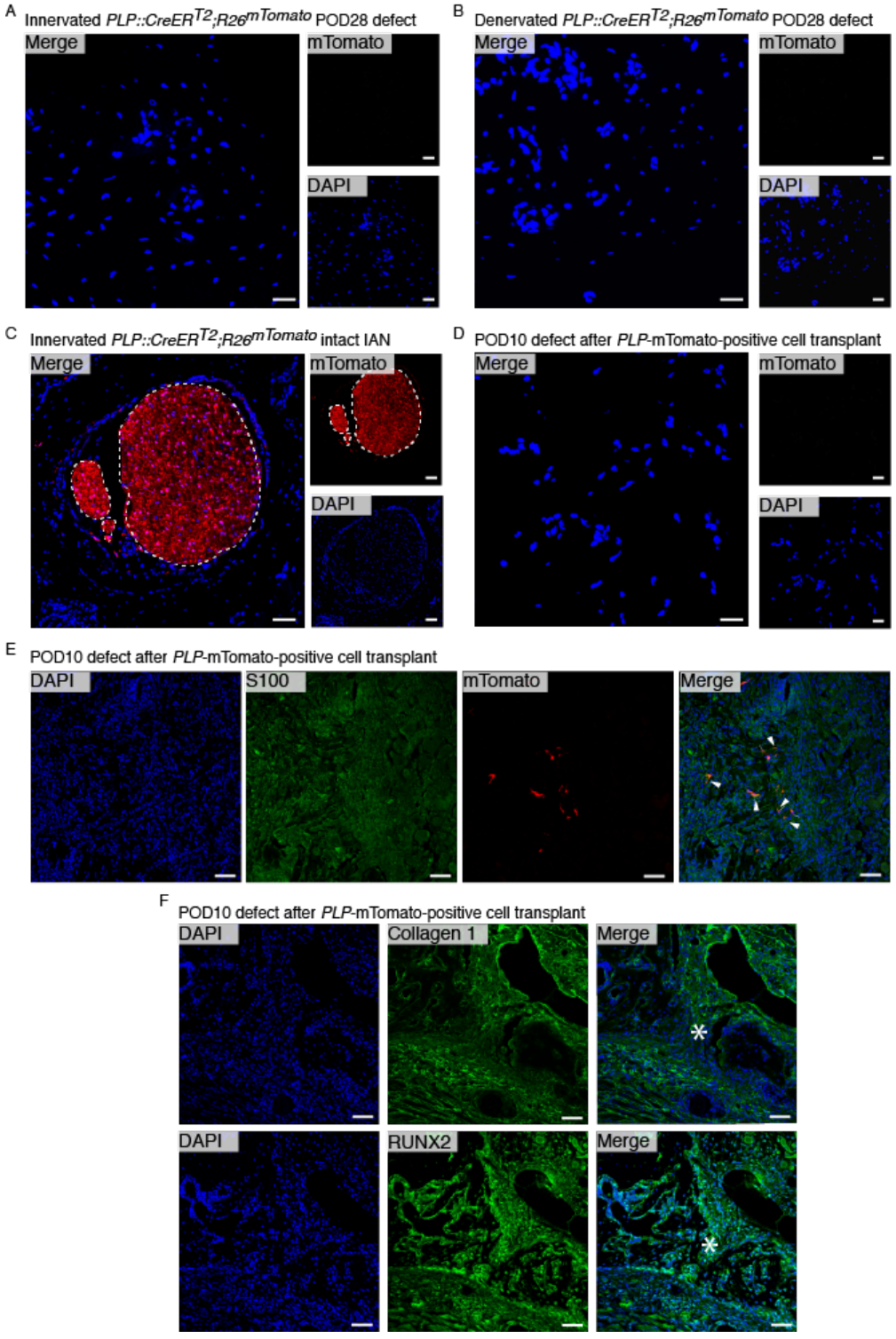

Supplemental Figure 3: Related to Figure 4. Lineage tracing of *PLP*-mTomato-positive Schwann cells *in vivo* and after transplantation.

(A, B) Lineage tracing of innervated (A) and denervated (B) healing defects harvested 4 weeks after osteotomy in PLP Tomato mice. No *PLP*-mTomato-positive cells are visualized in the healed bone. (n = 3 biological replicates)

(C) A positive control for *PLP* expression in PLP Tomato mice (intact IAN) is included for reference. The IAN is outlined with the white dotted line. (n = 3 biological replicates)

(D) Healing bone of denervated NOD-SCID mouse 10 days after defect creation and transplantation of *PLP*-mTomato-positive Schwann cells. No *PLP*-mTomato-positive cells are visualized in the healing bone. (n = 5 biological replicates).

(E) The identity of *PLP*-mTomato-positive cells after transplantation into healing denervated mandibular defects was investigated with immunohistochemical staining for S100. Co-staining of mTomato and S100 revealed that transplanted cells maintain identity as Schwann cells post-transplantation. Double positive cells are indicated with white arrows (right panel).

(F) After transplantation of *PLP*-mTomato-positive cells into healing denervated mandibular defects, the presence of repaired bone was confirmed with staining for markers associated with bone formation. Collagen 1 and *RUNX2* were positively identified in healing bone post Schwann cell transplant. The asterisk marks the center of the bone defect.

Scale bars, 100 μm (A, B, D,E,F) and 200 μm (C)

Supplemental Figure 4

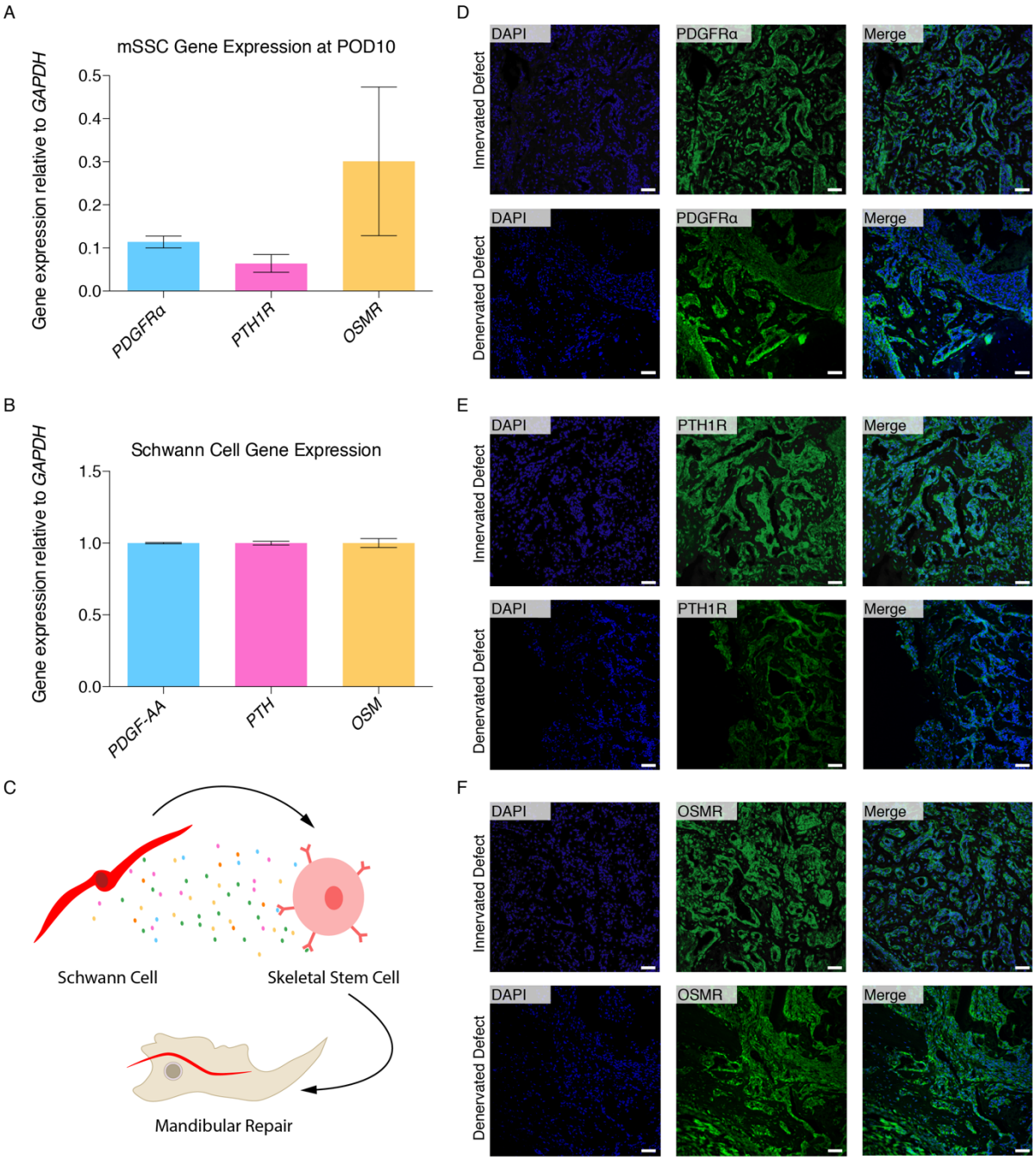

Supplemental Figure 4. Related to Figure 4. Suggested mechanism for mSSC and Schwann cell circuitry during mandibular healing.

(A) RT-qPCR confirmed expression of *PDGFRα*, *PTH1R*, and *OSMR* genes by mSSCs isolated from innervated mandibles 10 days after osteotomy. Gene expression is normalized to uninjured, innervated mandible gene expression and *GAPDH*. This experiment was performed with 10 biological replicates and three technical replicates per condition.

(B) RT-qPCR confirmed expression of *PDGF-AA*, *PTH*, and *OSM* genes by Schwann cells isolated from innervated, uninjured mandibles. Gene expression is normalized GAPDH. This experiment was performed with 12 biological replicates and three technical replicates.

(C) Proposed mechanism for mSSC and Schwann cell circuitry during nerve dependent mandibular healing. Schwann cells secrete paracrine factors such as PDGF-AA, PTH and OSM to support mSSC proliferation and function, allowing them to enact mandibular repair. Signaling by additional paracrine factors likely also contributes to this mechanism and have yet to be studied.

(D, E, F) Immune staining (green) for PDGFRα (D), PTH1R (E), and OSMR (F) in innervated (top panels) and denervated (bottom panels) mandibular defects and counterstained with DAPI (blue) to confirm receptor presence in the tissue after osteotomy. This experiment was performed with 5 biological replicates per condition.

Scale bars, 50 μm (D, E, F)